## Application for United States Letters Patent

## To all whom it may concern:

Be it known that Anna Marie Pyle and Eckhard Jankowsky

have invented certain new and useful improvements in

## ASSAYS FOR EVALUATING THE FUNCTION OF RNA HELICASES

of which the following is a full, clear and exact description.

# Assays For Evaluating The Function Of RNA Helicases

5

The invention disclosed herein was made with Government support under NIH Grant No. RO150313 from the Department of Health and Human Services. Accordingly, the U.S. Government has certain rights in this invention.

10

## Background on the Invention

Throughout this application, various publications are referenced by author and date. Full citations for these publications may be found listed alphabetically at the end of the specification immediately preceding Sequence Listing and the claims. The disclosures of these publications in their entireties are hereby incorporated by reference into this application in order to more fully describe the state of the art as known to those skilled therein as of the date of the invention described and claimed herein.

20

25

30

15

RNA conformation is of elemental importance in RNAinduced catalysis, as well as RNA interactions with other cellular components. Many central components of gene expression and RNA metabolism occur in ribonucleoprotein complexes, most notably the ribosome spliceosome. Within these large complexes, alternative conformations of specific RNAs have been demonstrated and the alteration of RNA conformation is believed to play a critical role in enabling, driving and assuring the fidelity of the catalytic reactions these complexes perform (Staley and Guthrie, 1998). Therefore, understanding the factors capable of inducing RNA conformational alterations within these complexes is likely to be central to an overall appreciation of

10

15

20

25

mechanisms by which they execute their intricate and demanding functions.

By exploring the effect of the duplex length of the substrates on the unwinding reaction under defined reaction conditions, the response of unwinding rate and amplitude to the duplex length can provide information about processivity and directionality (Fig. 1). the requirements for an experimental setup to probe and quantify processivity and directionality are to develop a substrate system where only the duplex length is variable and, using this substrate system, establish experimental conditions where rate and/or amplitude provide information about processivity and directionality.

RNA helicases of the DExH/D family play an essential role in viral replication and cellular RNA metabolosim, including central functions in RNA splicing, translation regulation of gene Despite expression. importance of these proteins, their RNA helicase activity has not been subjected to enzymological study. knowledge of cellular metabolism is therefore constrained by a limited understanding of reaction mechanism by motor proteins in the RNA helicase family. To address this problem, mechanistic studies have been initiated on two viral DExH/D proteins which are part of the RNA helicase family: NPH-II from Vaccinia and NS3-4A from Hepatitis C (HCV). The NPH-II protein is shown to be a processive, directional RNA helicase with specific roles for both the binding and hydrolysis of ATP. established qualitative features of NPH-II activity, the use of direct and stopped-flow kinetic methods to determine the quantitative kinetic parameters such as

10

15

20

25

translocation rates, reaction step size, processivity, helicase binding, ATP binding and hydrolic rate constants that describe the framework for catalytic activity of this prototypical RNA helicase. All aspects of cellular RNA metabolism and processing involve DExH/D proteins, which are a family of enzymes that unwind or manipulate RNA in an ATP-dependent fashion (de la Cruz, et al., DExH/D proteins are also essential for the replication of many viruses, and therefore provide targets for the development of therapeutics (Radare and Haenni, 1999). All DExH/D proteins characterized to date hydrolyse neucleoside triphosphates and, in most cases, this activity is stimulated by the addition of RNA or Several members of the family unwind RNA duplexes DNA. in an NTP dependent fashion in vitro (de la Cruz, et al., 1999 and Wagner, et al., 1998); therefore it has been proposed that DExH/D proteins couple NTP hydrolysis to RNA conformational change in complex macromolecular assemblies (Stanley and Guthric, 1998). Despite the central role of DExH/D proteins, their mechanism of RNA helicase activity remains unknown. It is shown that the DExH protein NPH-II unwinds RNA duplexes in a processive, unidirectional fashion with a step size of roughly onehalf helix turn and that there is a quantitative connection between ATP and helicase processivity, thereby providing direct evidence that DExH/D proteins can function as molecular motors on RNA.

#### Summary of the Invention

The present invention provides a method for detecting the release of a single-stranded RNA from an RNA duplex which comprises: (a) admixing an RNA helicase with the RNA duplex under conditions permitting the RNA helicase to unwind the RNA duplex and release single-stranded RNA, wherein the RNA duplex comprises a first RNA having a first label attached thereto and a second RNA, such first label being capable of producing a luminescent energy pattern when the first RNA is present in the RNA duplex differs from the luminescent energy pattern produced when the first RNA is not present in the RNA duplex, (b) subjecting the admixture to conditions which permit (i) the RNA helicase to unwind the RNA duplex and release single-stranded RNA, and (ii) the first label to produce luminescent energy; and (c) detecting a change in the luminescent energy pattern produced by the first label so as to thereby detect release of single-stranded RNA from the RNA duplex.

5

10

15

10

15

2.0

25

30

5

## Breif Description of the Figures

#### Figure 1

Kinetic approach to probe processivity and directionality of the unwinding reaction. Unwinding of a dsRNA is the reverse reaction of the association of two complementary Thus, unwinding occurs only when so many basepairs are disrupted that no nucleation locus can Practically, that means that unwinding is only observed, when less then 4 or 3 basepairs remain in the This emphasizes that by monitoring a duplex unwinding reaction one actually monitors the very last event of the strand separation process.

A processive reaction occurs in distinct consecutive steps, therefore, there are reaction intermediates (I) until the reaction product (P) is formed. For a nonprocessive reaction (for instance if the unwinding occurs in one power stroke) there are no intermediates. the experimental rationale for probing processivity is to determine whether there are reaction intermediates or If the reaction proceeds in distinct consecutive translocation steps, the translocation is rate limiting for the unwinding reaction, and the rate constants  $(k_{\rm tr})$ of these translocation steps are of similar or equal size, intermediates (I) would accumulate. This would be reflected in a lag phase in the unwinding timecourse of the product (P) formation. With increasing duplex length more reaction intermediates would appear and timecourses would display a greater lag phase with increasing duplex length. The number of intermediates  $(I_{1...n})$  is indicative for the number of kinetic steps that the helicase takes to unwind a duplex of given length. More intermediates cause also more dissociation "events", provided that these intermediates are susceptible to dissociation. This is

10

15

20

25

30

determined by the ratio of the translocation rate  $(k_{tr})$  to the respective dissociation rate constant constant  $(k_{di})$  (Ali and Lohmann, 1997). If a measurable fraction of protein dissociates during each unwinding step, the reaction amplitude should decrease with increasing duplex length. This should also occur when the translocation is not rate-limiting for the unwinding reaction. However, in that case the duplex length should not affect the reaction rate. If the reaction is not processive, there should be under no conditions a sensitivity of either reaction rate or amplitude to the length of the duplexes.

Probing the processivity is the prerequisite for testing the directionality of the unwinding, since only a The processive reaction can be directional. directionality can be directly tested by monitoring at least one reaction intermediate and the reaction product at the same time under conditions where the translocation the unwinding reaction. The experimental conditions for probing processivity and directionality have to be chosen in a way, that all RNA is complexed with protein at the reaction start and that dissociation of the protein off the RNA substrate is irreversible.

#### Figure 2

Unwinding of various RNA substrates by NPH-II. Unwinding reactions were performed in a reaction buffer comprising  $30\mu\text{L}$  volume (40mM Tris.Cl, pH 8.0, 2mM DTT, 20mM NaCl, 3mM MgCl<sub>2</sub>, 3mM ATP, 16nM NPH-II, 3nM RNA substrate) at 23 C. Protein, RNA substrate, and MgCl<sub>2</sub> were incubated in reaction buffer prior to the reaction for 7 min. The reaction was started by addition of ATP. Aliquotes were

10

15

20

25

withdrawn at appropriate times and added to two volumes quenching buffer (25mM EDTA, 0.4% SDS, 10% glycerol, 0.05% BPB, 0.05% XCB). This mixture was immediately cooled on ice. After the last aliquot was taken, the samples were applied to 15% native PAGE.

#### Figure 3

Effect of trap RNA on unwinding reactions. (A) Since reactions are performed with preannealing of protein and RNA prior to the reaction, the protein-RNA complex [ES] is already formed at the reaction start. As protein dissociates from the RNA substrate during the unwinding reaction, re-binding of the protein and multiple reaction Binding ("trapping") free protein cycles can occur. during the course of unwinding prevents re-binding during the reaction. Complete "trapping" of all free protein is ensured by using a large excess of RNA (trap RNA) (B) Effect of trap compared to the duplex substrate. addition on reactions with LS83 and LS36. conditions were as described in Fig. 2, except that the ATP was pre-mixed with the trap RNA (39-mer RNA oligo) and the reaction was started with this ATP/trap mixture. The trap concentration in the reaction was 600nM which is Higher the substrate. fold excess over concentrations of trap did not change the observed The substrate was bound to 100% of the timecourses. protein prior to the reaction as verified by gel shift analysis of the RNA protein complexes (not shown).

#### 30 Figure 4

Monitoring duplex unwinding by fluorescence energy transfer. (A) Both strands of the duplex are labeled with a fluorescence transfer donor-acceptor-pair of fluorescent dyes. The top strand is labeled with

10

15

20

25

flourescein (donor) at the 3' -end and the bottom strand is labeled with rhodamin (acceptor) at the 5' -end. attached fluorescein is excited at 492nm. Due to the proximity of the acceptor label in the duplex, emission of the fluorescein label is quenched. Upon unwinding, both labels depart from each other, quenching of the fluorescein label no longer occurs and of the fluorescein emission in the increase unwinding be detected. (B) The can fluorescence reactions were performed as described in Fig. 3, but in a volume of  $600\mu L$  in a fluorescene cuvette. fluorescence intensity was measured at defined intervals (small points). The resulting curve was corrected for the reaction amplitude derived by gel shift measurements of identical reactions and both, the derived fluorescence curve and the measurements from gel shift experiments (large points) are overlaid in the plots. Reactions were performed with US18 (18bp duplex region) and US36 (36bp duplex region).

#### Figure 5

Effect of ATP concentration on the unwinding reaction. Unwinding reactions with LS36 were performed as described in Fig. 3 (pre-annealing, trap addition). The plot shows the final amplitude of the reaction versus the respective ATP concentration. Amplitude values were determined out of 8 aliquotes taken from the reaction.

#### Figure 6

Effect of  $\mathrm{Mg}^{2+}$  substitution on the unwinding reaction. Timecourses with US36 were measured as described in Fig. 3 (trap RNA, pre-annealing), except that 3nM  $\mathrm{Mg}^{2+}$  (A) was substituted with 3mM  $\mathrm{Mn}^{2+}$  (B) and 3mM  $\mathrm{Co}^{2+}$  (C). The left panels show the gel printouts of the reactions that are

10

15

20

25

30

plotted on the right panels as fraction unwound substrate versus time.

#### Figure 7

Effect of the duplex length on unwinding reactions in the presence of Co<sup>2+</sup>. Unwinding reactions were performed with US36 (36bp duplex region) and US18 (18bp duplex region) under the conditions described in Fig. 6. The solid lines represent fits for a consecutive 2 step reaction with equal rate constants (Ali and Lohmann, 1997) for the 18bp duplex and for a consecutive 4 step reaction with equal rate constants for the 36bp duplex.

#### Figure 8

Probing the directionality of the unwinding reaction by using multi-piece substrates. (A) Multi-piece substrates were generated by site directed processing of the top strand RNA with an engineered DNAzyme (Santoro and Joyce, 1997) and subsequent hybridization of the two "pieces" with the bottom strand. (B) Unwinding reactions of MPS 36/75 (36nt oligo binds next to the single stranded overhang and 75nt oligo binds adjacent to this strand) and MPS 83/28 (83nt oligo binds next to the single stranded overhang and 28nt oligo binds adjacent to this strand) in the presence of  $Mg^{2+}$  were carried out as The fraction of the displaced described in Fig. 3. pieces was calculated according to frac[N]  $_{\rm t}$  = [N  $_{\rm t}/$  (N  $_{\rm t}$  +  $\rm M_t + S_t)] \star [(N_{\infty} + M_{\infty} + S_{\infty})/N_{\infty}]$ , where frac[N]  $_t$  is the fraction of the respective "piece" at the time t;  $N_{\rm t}$  is the intensity of the band of the "piece" N at the time t;  $\mathrm{M}_{\mathrm{t}}$  is the intensity of the band of the "piece"  $\mathrm{M}$  at the time t; St is the intensity of the not unwound substrate band at the time t;  $N_{\scriptscriptstyle \infty}$  is the intensity of the band of

10

15

20

25

30

N after heat denaturation;  $M_{\infty}$  is the the "piece" intensity of the band of the "piece" M after heat denaturation and  $S_{\infty}$  is the intensity of the not unwound substrate band after heat denaturation. S<sub>∞</sub> is, however, The solid lines represent a fit of the usually zero. timecourse to a rate law describing a sum of two first order reactions. (C) Reactions of MPS 36/75 and MPS 83/28 in the presence of  $\operatorname{Co}^{2+}$  were performed as described in The fraction of the displaced pieces were calculated as described above. The solid lines represent fits of the timecourses to rate laws describing a consecutive 4 step reaction for T36, a 12 step reaction for T75 and T28 and a 9 step reaction for T 83, using equal rate constants for the steps, respectively.

Figure 9

Kinetics of duplex unwinding. Reactions in the presence (open circles) and absence (filled circles) of trap RNA with a 36-bp substrate (a) and a 83-bp substrate (b). The 83-bp substrate is an extension of the 36-bp substrate. The fraction of unwound substrate (indicated on the y axis) was fitted to the integrated first-order rate law using Kaleidagraph software (Abelbeck). Rate constants (k) and reaction amplitudes (A) in the absence of trap RNA:  $k = 3.5 \pm 0.1 \, \text{min}^{-1}$ , A = 0.96, 36 - bp substrate;  $k = 3.4 \pm 0.1 \, \text{min}^{-1}$ , A = 0.97, 83 - bp substrate. In the presence of trap RNA:  $k = 3.6 \pm 0.2 \, \text{min}^{-1}$ , A = 0.77, 36 - bp substrate;  $k = 3.6 \pm 0.3 \, \text{min}^{-1}$ , A = 0.52, 83 - bp substrate. Variances are standard deviations from the fit.

Figure 10

Estimation of the unwinding step size. Time courses of substrates containing duplex regions of 12 (open squares), 18 (filled squares), 24 (open circles) and 36

(filled circles) bp unwound by NPH-II in the presence of  $4mM\ CoCl_2.$  Substrates contain a 35-U single-strand overhang 3' to the duplex region. Step size and the unwinding (translocation) rate constant were calculated were calculated from at least two independent time courses for each duplex which are overlaid on the plots. Solid lines are best fits to the kinetic model resulting in an unwinding step size of 6 bp and an average unwinding rate constant of  $k_g=13.4\pm0.8\ min^{-1}.$ 

10

15

20

5

#### Figure 11

Probing helicase directionality with multiplece substrates (MPS)  $\bf a$ , Design of the MPS  $\bf b$ . Unwinding of MPS in 4mM MgCl<sub>2</sub> and trap RNA. Unwinding rate constants were similar for all pieces (k=3.3 ± 0.5 min<sup>-1</sup>); reaction amplitudes (A) were MPS 36/75, T36 A=0.74; T75, A = 0.32; MPS 83/28, T83, A=0.43; T28, A=0.27.  $\bf c$ . Unwinding of multiplece substrates in 4 mM CoCl<sub>2</sub> and trap RNA. Kinetic data were analysed as described in Fig. 2, which resulted in average values of  $k_g = 12.4 \pm 2.1$  min<sup>-1</sup> and a step size of 6pb, consistent with the values obtained for oligomers shown in Fig. 2.

#### Figure 12

Processivity of NPH-II a, ATP dependence of processivity 25 in 4 mM  ${\rm MgCl_2}$  (filled circles) and 4mM CoCl The solid line is a hyperbolic fit: P = circles). saturation; Zis ATP processivity at concentration where P =  $P_{\infty}/2$ . In 4mM CoCl<sub>2</sub>,  $P_{\infty}$  = 1.00 ± 30 0.03 and Z = 0.50  $\pm$  0.06 mM. In 4mM MgCl<sub>2</sub>,  $P_{\infty}$  = 0.99  $\pm$ Processivities were 0.01 and  $Z = 0.14 \pm 0.01$  mM. determined from the reaction amplitudes of four duplexes

10

15

20

25

30

(12, 18, 24 and 36 bp, Fig. 2) at the ATP concentrations indicated. Amplitudes were obtained from at least three independent experiments. Processivity was calculated by fitting plots of amplitude at constant ATP concentration versus duplex length to Equation 2 using a step size of m=6 (Fig. 2). **b,c**, Dependence of reaction amplitude on ATP concentration for substrates with duplex regions of (filled circles), 18 (open circles), 24 squares) and 36 (open squares) basepairs in 4 mM  $MgCl_2$ Each reaction amplitude was (b) and  $4mM CoCl_2$  (c). determined in triplicate and the deviation from these independent measurements is indicated by the error bars. The solid lines are fits to equation 1, where  $k^{'}_{\ d}$  was assumed to equal  $K_{\scriptscriptstyle m}$  from multiple turnover ATPase measurements (1.1 mM in  ${\rm Mg}^{2^+}$  and 3.5 mM in  ${\rm Co}^{2^+}$  (Shuman, 1993; Gross and Shuman 1996), the step size was 6bp (Fig. 2), and  $k_{\text{p}}/k_{\text{U[S]}} \, \text{was allowed to flout.} \quad \text{In both Mg$^{2+}$ and Co$^{2+}$}$  $k_p/k_{U(S)} = 0.12$ .

#### Figure 13

The kinetic scheme for RNA helicase activity by NPH-II. Unwinding initiation and two unwinding/translocation  $\mathrm{ES}_1$  and  $\mathrm{ES}_2$  represent the enzyme steps are depicted. substrate complex in non-ATP-bound states, while  $[ES_1-$ ATP] and [ES2-ATP] represent ATP-bound states. Note that ATP is bound but indicates that 'ATP-bound' hydrolysed, whereas 'non-ATP-bound' indicates that no nucleotide is bound or that ADP and/or inorganic phosphate are bound. The equilibrium between ATP-bound compared non-ATP-bound fast is states and translocation with the unwinding rate constant  $k_{\text{U(S)}}$   $.\,k_{\text{P}}$ (Shuman, 1993; Gross and Shuman, 1996) is the rate constant for enzyme dissociation from subtrate in the ATP-free state, dissociation in the ATP-bound state is not significant (Fig. 4a)  $k_1$  is the rate constant for the unwinding initiation step. Reactions were conducted in the presence of trap-RNA (Fig. 1), thus ES dissociation is irreversible.

10

15

20

## Detailed Description of the Invention

The present invention provides an a method for detecting the release of a single-stranded RNA from an RNA duplex which comprises (a) admixing an RNA helicase with the RNA duplex under conditions permitting the RNA helicase to unwind the RNA duplex and release single-stranded RNA, wherein the RNA duplex comprises a first RNA having a first label attached thereto and a second RNA, such first label being capable of producing a luminescent energy pattern when the first RNA is present in the RNA duplex which differs from the luminescent energy produced when the first RNA is not present in the RNA duplex, (b) subjecting the admixture to conditions which permit (i) the RNA helicase to unwind the RNA duplex and release single-stranded RNA, and (ii) the first label to produce luminescent energy, and (c) detecting a change in the luminescent energy pattern produced by the first label so as to thereby detect release of single-stranded RNA from the RNA duplex.

In accordance with the present invention conditions which permit the RNA helicase to unwind the RNA duplex and release single-stranded RNA preferably include, but are not limited to the presence of ATP and a divalent cation, which preferably may be  $Mg^{2+}$ ,  $Mn^{2+}$  or  $Co^2$ .

The foregoing method may be carried out in numerous ways which will be readily understood by those skilled in the art. In a presently preferred embodiment of the invention the method utilizes a second label attached to the second RNA such that the luminescent energy produced by the first label interacts with the second label to produce a characteristic pattern when the first and second RNA are present in an RNA duplex, but interacts

30

10

15

20

25

differently or not at all when the RNA duplex unwinds. In one embodiment of the invention the first label is covalently attached at the 5' end of the first RNA and the second label, if any, is attached at the 3' end of the second RNA.

In accordance with the foregoing, embodiment the first and second label may comprise different fluorophors having the characteristic that the second label absorbs luminescent energy released from the first fluorophor when it is induced to emit luminescent energy by exposure to a particular type of radiation such as ultraviolet light of a defined wavelength. In one embodiment the first label is fluorescein isothiocyanate and the second label is rhodamine isothiocyanate.

As used herein luminescent energy includes but is not limited to fluorescence, phosphorescence, and chemiluminescence.

In the practice of the methods of the invention the compound capable of inhibiting unwinding activity of an RNA helicase may be a chemically synthesized substrate that preferentially binds over a endogenous substrate to the RNA helicase. In one embodiment of the invention the compound inhibits the accessibility of the ATP to the binding site on the protein thereby enabling the helicase to dissociate from the RNA at appropriate times. In another embodiment of the invention the compound induces a rate-limiting step by blocking and deblocking initiation of the RNA unwinding by the RNA helicase.

In the practice of the methods of the invention the compound capable of inhibiting the unwinding activity of an RNA helicase is present at a concentration capable of

35

inhibiting the unwinding activity of an RNA helicase. Accordingly, the effective amount will vary with the helicase used.

This invention also provides a method of measuring the rate of release of a single-stranded RNA from an RNA duplex which comprises detecting whether the single-stranded RNA is released from the RNA duplex at predetermined time intervals according to the method and determining therefrom the rate of release of the single-stranded RNA from the RNA duplex.

Furthermore, this invention provides a method of determining whether a compound is capable of modulating the release of a single-stranded RNA from an RNA duplex by an RNA helicase which comprises detecting the release of the single-stranded RNA from the RNA duplex according to the method wherein the compound is added to the mixture of RNA duplex and RNA helicase

Still further, this invention also provides effective amounts of compounds capable of inhibiting unwinding activity of an RNA helicase together with suitable emulsifiers, diluents, preservatives, solubilizers, adjuvants and/or carriers useful in treatment of viral RNA helicase or a viral Hepatitis C. Such compositions otherwise dried lyophilized or or are formulations and include diluents of various buffer content (e.g., Tris-HCl., acetate, phosphate), pH and ionic strength, additives such as albumin or gelatin to prevent absorption to surfaces, detergents (e.g., Tween bile acid Pluronic F68, 80, Tween (e.g., glycerol, polyethylene agents solubilizing glycerol), anti-oxidants (e.g., ascorbic acid, sodium metabisulfite), preservatives (e.g., Thimerosal, benzyl

20

25

30

35

5

10

10

15

2.0

25

30

bulking substances or tonicity parabens), alcohol, modifiers (e.g., lactose, mannitol), covalent attachment of polymers such as polyethylene glycol to the compound, complexation with metal ions, or incorporation of the compound into or onto particulate preparations polymeric compounds such as polylactic acid, polglycolic acid, hydrogels, etc, or onto liposomes, micro emulsions, multi lamellar unilamellar or micelles, erythrocyte ghosts, or spheroplasts. Such compositions will influence the physical state, solubility, stability, rate of in vivo release, and rate of in vivo clearance of the compound. The choice of compound will depend on the physical and chemical properties of the compound capable of alleviating the symptoms of a viral RNA infection.

This invention is illustrated in the Experimental Details section which follows. These sections are set forth to aid in an understanding of the invention but are not intended to, and should not be construed to, limit in any way the invention as set forth in the claims which follow thereafter.

## Experimental Details

The DExH helicase NPH-II from vaccinia virus (Shuman, 1992) was subjected to quantitative kinetic analysis that varied in composition and length. Kinetics of unwinding were monitored using gel-shift electrophoresis fluorescence energy transfer methodologies. substrates contained a single-strand 3' overhang, which is required for NPH-II unwinding activity (Shuman, 1993). The single-strand 3' overhang was identical in length and sequence for every substrate (Fig. 9). single-turn-over preformed under were reactions conditions with respect to the RNA substrate. A large

10

15

20

25

excess of nonspecific trap RNA (de la Cruz, 1999) was added to prevent helicase from reassociating with duplex once it falls off during the course of reaction.

In the absence of trap RNA, the unwinding rate and reaction amplitude (defined as the final fraction of unwound RNA) were both insensitive to duplex length (Fig. Each reaction was first-order with a rate constant of 3.5  $\pm$  0.2 min<sup>-1</sup> (Fig. 9). In the presence of trap RNA, the rates remained independent of duplex length however, the reaction amplitude decreased with increasing duplex These observations provide three length (Fig. 9). mechanistic insights. First, the fact that long duplexes can be unwound at all in the presence of trap RNA provides strong qualitative evidence that the helicase is a processive enzyme consistent with previous multipleturnover studies. Second, the dependence of amplitude on duplex length indicates that more protein dissociates RNA substrate when the duplex is indicating that more protein dissociates from an RNA substrate when the duplex is longer, indicating that more unwinding steps may be required for a long duplex, and there is a specific degree of processivity for the NPH-II Last, the similar rates observed for enzyme (Fig. 9). the unwinding of different duplex lengths indicate that individual unwinding steps do not limit the reaction rate Rate-limiting events during under these conditions. translocation would result in a length-dependent lag phase in each time course.

To evaluate helicase step size and to provide an additional proof of processivity, it was necessary to monitor individual unwinding steps. Conditions were sought under which helicase translocation becomes rate limiting. Variation in temperature and pH did not cause

30

10

15

20

25

30

the rates to become increasingly sensitive to duplex length (E. Jankwsky et al., unpublished data); however, marked effects were observed when  $Mg^{2+}$ , which is the cofactor for ATP hydrolysis, was replaced by Co<sup>2+</sup>. unwinding reactions displayed pronounced lag phases which increased incrementally with the duplex length (Fig. 10). The data were fit numerically to a kinetic model that relates the translocation rate constant to step size and duplex legngth (Material and Methods). analysis, the unwinding step size of NPH-II was estimated to be six base pairs (bp) and the unwinding rate constant in Co<sup>2+</sup> step at each translocative concentration of 3.5 mM),  $k_n$ , was 13.4  $\pm$  0.8 min<sup>-1</sup>. Using the step size of 6 bp, it is possible to calculate a lower limit for the translocation rate constant in Mg<sup>2+</sup>. In these conditions, k, was greater than 350 min<sup>-1</sup>, indicating that translocation in  $Mg^{2+}$  is at least 25-fold faster in  $Co^{2+}$ . The slower unwinding rate in  $Co^{2+}$  is not attributable to inhibition of ATPase activity, as kinetic parameters for hydrolysis of ATP are similar in Co2+ and Mg<sup>2+</sup> (E. Jankowsky et al., unpublished data).

The existence of a defined step size indicates regularity in the translocation process; that is, unwinding is not random with respect to individual translocation rates and the number of bp displaced in one unwinding step. The step size obtained herein corresponds to about half of a helical turn and is very similiar to the unwinding step size of the UvrD DNA helicase of 4 - 5 bp (Ali and Lohmann, 1997). It is important to note that the unwinding step size is an average value that may not necessarily reflect actual microscopic translocation steps of a helicase (Ali and Lohmann, 1997).

10

15

20

25

30

35

Although the above results suggest that RNA unwinding occurs in consecutive steps, the assays that we used are designed to monitor only the very last event in strand displacement (one does not see a signal until the duplex is completely unwound). Therefore, it is impossible to directional translocation distinguish between translocation that occurs through random facilitated diffusion (Shimamoto, 1999; Kelemen and Raines, 1999). To determine which of these mechanisms applies, detection of an unwinding intermediate was needed. accomplished by using multipiece substrates (MPS), consisting of a continuous bottom strand that is annealed to two adjacent pieces of top-strand RNA (Fig. 3a). pieces were generated by site-specific top-strand cleavage of a single continuous piece of top-strand RNA (Fig. 11a). The top-strand (first RNA molecule) pieces were generated by site-specific cleavage of a single continuous piece of top-strand RNA using synthetic DNAzyme endonucleases (Santoro and Joyce, 1996). had different lengths and could resultant pieces by their distinguished respective therefore be electrophoretic mobilities (Fig. 11b, 11c). the results from being biased by the relative length of the top-strand pieces we designed two different sets of All MBPS unwinding reactions were 11a). (Fig. carried out under single-turnover conditions with respect to the RNA substrate, and in the presence of trap RNA.

NPH-II unwound both sets of MPS (Fig. 11b), indicating that the helicase can proceed through nicks in the top strand of the substrate. In the presence of  $Mg^{2+}$ , all pieces were displaced with apparent first-order kinetics with similar rate constants,  $k=3.3\pm0.5~\text{min}^{-1}$  (Fig. 11b). For both sets of MPS, the piece that was bound farthest from the overhang was displaced with a lower

amplitude than the piece located closer to the single-strand 3' overhang (Fig. 11b). This implies that fewer unwinding steps were required for the displacement of the piece closer to the overhang. The fact that these effects depend exclusively on the location of the top strands relative to the single-strand 3' overhang (rather than their length) strongly suggests that the strand displacement progresses in a distinct 3'-to-5' direction with respect to the bottom strand.

The similar unwinding rates for both pieces of top-strand RNA indicate that neither a late step in the reaction, such as the final strand separation, nor translocation itself, limits the rate of the overall process in  $\mathrm{Mg}^{2^+}$ . A late rate-limiting step would result in a slower rate for unwinding of the piece farthest from the overhang because two strand separations are required for unwinding of the second piece. A rate-limiting translocation would cause a lag phase in the time courses as observed in the presence of  $\mathrm{Co}^{2^+}$  (Fig. 10). Thus in the presence of  $\mathrm{Mg}^{2^+}$ , an initiation step at the very begining of the unwinding process limits the rate of the overall

reaction.

By contrast, reactions conducted in the presence of Co<sup>2+</sup> displayed a pronounced lag phase attributable to ratelimiting translocation steps (Fig. 11c). Notably, the displacement of the two pieces occurred with different lag phases. The lag was largest for the piece farthest from the overhang, reflecting an increase in the number of unwinding steps that are required as the helicase moves away from the single-strand 3' overhang. The effects were exclusively dependent on the location of the pieces relative to the over hang and not on their length indicating a distinct 3'-to-5' directionality in the

10

15

20

25

30

35

progression of unwinding with respect to the bottom strand.

Having established that the helicase unwinds substrates in a processive directional fashion with a distinct unwinding step size it was of interest to correlate this process with the role of ATP. The effect of ATP on enzyme processivity (P) was of particular Processivity reflects (Fig. 12). interest probability that the helicase will perform the next unwinding step rather than dissociate from the substrate Ouantitation 1996). (Lohmann and Bjoernson, processivity was carried out by determining the reaction amplitude in the presence of trap RNA, such that all dissociation of protein from the RNA substrate during unwinding was effectively irreversible. Processivity decreased with decreasing ATP concentration (Fig. 12a), which indicates that the helicase dissociates more readily from RNA in non-ATP-bound states than in the ATPbound state, consistent with previous studies of RNA In addition, binding by NPH-II (Shuman, 1992). processivity at ATP saturation approaches P = regardless of whether  $Co^{2+}$  or  $Mg^{2+}$  are the cofactors for ATP hydrolysis (Fig. 12a). This indicates that NPH-II in the ATP-bound state does not significantly dissociate from the RNA substrate, and that dissociation of protein from RNA occurs predominantly in non-ATP-bound states. This is highly instructive because it shows that ATP binding and not just the consumption of ATP through hydrolysis, is of critical importance in the helicase mechanism.

Although RNA unwinding activity by NPH-II is dependent on ATP hydrolysis (Shuman, 1992), one must establish quantitative link between ATP utilization and a specific

amount of unwinding to conclude that DExH/D proteins behave as true molecular motors (Schnapp, 1995). Plots of reaction amplitude versus ATP concentration resulted in sigmoidal curves (Fig. 12b, 12c) that are affected by duplex length: the longer the duplex, the more pronounced the sigmoidal shape of the time course. These results, together with the observation of a discrete step size and the fact that NPH-II does not dissociate in the ATP-bound state are consistent with the kinetic scheme shown in Fig. 13. This scheme was used to derive an explicit equation that describes the plots of reaction amplitudes versus ATP concentration (Fig. 12b, 12c).

$$A = (1 - x) \cdot \left(1 + \frac{k_c}{k_{U(S)}} \cdot \frac{K'_d}{[ATP]}\right)^{-Um}$$

The fit of this expression to the data establishes a direct relationship between processivity and ATP concentration, indicating that translocation is coupled to the binding of ATP. This link between ATP utilization and directional movement supports the assertation that NPH-II is a processive molecular motor.

The results suggest the following basic mechanism for RNA duplex unwinding by the DExH RNA helicase NPH-II (Fig. 13); unwinding is preceded by a slow initiation step (2.3  $\pm$  0.2 in Co<sup>2+</sup>, 3.5  $\pm$  0.3 in Mg<sup>2+</sup>). Subsequent unwinding occurs in distinct consecutive steps of roughly one-half helix turn in a defined 3'-to-5' direction with respect to the single-strand 3' overhang. The helicase

10

15

2.0

25

30

35

translocates rapidly along the RNA substrate, unwinding RNA with a rate that is dependent on identity of the metal ion cofactor (13.4  $\pm$  0.8 min<sup>-1</sup> per step for Co<sup>2+</sup>;  $\geq$ 350  $min^{-1}$  per step for  $Mg^{2+}$ ). During each step, a fraction of protein, predominantly in non-ATP-bound states, dissociates from the RNA. The dependence of reaction on ATP hydrolysis and the direct connection between ATP binding and translocation indicate that NPH-II is a processive directional motor for unwinding RNA. This activity DexH/D proteins might ensure processive, rearrangement of structured RNA requlated macromolecular assemblies during processes such as RNA splicing, export or translation initiation. limiting step before translocation would provide a straight-forward way to control unwinding by blocking and deblocking an early initiation event. Alternatively, factors that control the local concentration of ATP or accessiblity of the ATP binding site on the protein could enabling the helicase processivity, dissociate from RNA at appropriate times.

DEXH/DEAD box proteins (putative RNA helicases) are important in all aspects of RNA transcription, maturation and translation. A step towards understanding the function(s) of this class of enzymes at the molecular level is to investigate the mechanism underlying duplex RNA unwinding by the vaccinia virus DEXH RNA helicase NPH-II.

Transient kinetic experiments were performed using a series of fluorescent dye labeled RNA substrates with duplex regions of different length. The unwinding reaction was monitored continuously in real time by measuring the changes in fluorescence energy transfer upon the unwinding reaction.

Timecourses under single turnover conditions displayed significant dependence on the length of the duplex region in terms of reaction rate and reaction amplitude. Reaction rates were also affected by the nature of the divalent cation cofactor. In the presence of Co<sup>2+</sup> timecourses were found to have a significant lag phase, increasing with the duplex length. In the presence of Mg<sup>2+</sup> no comparable lag phase was observed, but reaction rate as well as reaction amplitude were greater as compared to the reactions with Co<sup>2+</sup>. Dependent on the duplex length, the ATP concentration affected the reaction rate and amplitude with both metal cofactors.

These findings suggest a basic mechanism for the translocation/unwinding reaction consisting of consecutive events of ATP binding and translocation. Quantitative description of this mechanism leading to the rate and step size for the translocation/unwinding reaction follows.

Design of the RNA substrates. These studies used the RNA helicase, vaccinia virus DEXH protein NPH-II. The protein was expressed in baculavirus infected insect cells (Gross and Shuman,1995). The NPH-II helicase requires the substrate to have single stranded overhangs 3'-end to the duplex region (Shuman, 1992), which are necessary for the helicase to bind the substrate (Shuman, 1993). In order to prevent binding of the protein at multiple sites, a substrate for mechanistical studies should contain solely one single stranded region. This single stranded region should be constant for a series of substrates where the length of the duplex region is variable.

10

15

20

25

30

Two different ways to design the substrates: by chemical synthesis with subsequent template directed ligation (Moore and Sharp, 1992) and by in vitro transcription generated templates (Chabot, 1992) subsequent DNAzyme processing (Santoro and Joyce, 1997) in order to produce perfect blunt ended Chemical synthesis bears the advantage of complete flexibility in the sequence choice and allows incorporation of a variety of modifications including modifications as backbone nucleoside and The method is limited in terms of fluorescent labels. the length of the oligos which can be produced. In vitro transcription from PCR generated templates does not have these limitations for the length of the oligos but this method is not completely variable concerning the sequence and it does not allow the incorporation of extensive modifications.

Exploiting the respective advantages of both methods we designed two series of substrates. The series based on chemical synthesis contains a U-35 single stranded overhang and duplex regions from 12 to 36 basepairs (Fig. 2). The series based on *in vitro* transcription contains a 33 mucleotide overhang and duplex regions from 36 83 basepairs. The unwinding reaction of the substrates was monitored by separation of unwound strands from intact substrate on native gel electrophoresis. All substrates tested were unwound by NPH-II (Fig. 2).

Effect of trap RNA on the unwinding reaction. Excess single stranded RNA (Trap RNA) is required for single turnover reactions where dissociation of protein from the substrate has to be irreversible, i.e. trap RNA has to prevent re-binding of protein to the substrate during the

10

15

2.0

reaction (Fig. 3a). The effect of trap RNA addition with two substrates was tested: one with a 36bp duplex region and one with a 83bp duplex region. Reaction rates and amplitudes without trap addition were comparable with both substrates (Fig. 3b). The addition of trap RNA did not significantly change the reaction rates with both substrates. However, reaction amplitudes decreased with both of the substrates as compared to the reactions without trap (Fig. 3b), whereby the reaction amplitude with the longer substrate (LS83) was lower than the amplitude with the shorter substrate (LS36). Thus, the duplex length does not affect the rate of unwinding suggesting that the rate-limiting step for the overall which is not a potential is reaction an event different translocation. However, the reaction amplitudes indicate that protein dissociates off the substrate more frequently during the of unwinding of that the number longer duplexes, suggesting dissociation "events" increases with increasing duplex This is an indirect indication that there are distinct consecutive steps in the unwinding reaction, even if this is not reflected in the reaction rate (Fig. 1).

Monitoring duplex unwinding by fluorescence measurements. 25 In order to obtain data of higher time resolution, the unwinding reaction was monitored by measuring changes in fluorescence in real time upon the unwinding fluorescently labeled duplexes (Fig. 4a). Since the data fluorescence are obtained by gel shift and by 30 fluorescence method the real time superimposable, artifacts were also the control that no introduced by the gel separation method (Fig4b). reaction rates with both substrates tested (18bp duplex and 36bp duplex) were similar (Fig.4b). The reaction amplitude of the 36bp duplex was lower than that of the 18bp duplex. Thus, these observations agree with the data described above (Fig. 3)

5

10

15

20

25

the ATPconcentration the unwinding Effect of onThe decreasing reaction amplitude reaction. increasing duplex length in reactions where protein dissociation from the substrate was irreversible (Figs. 3 and 4) indicates that with each "unwinding step" a certain fraction of protein dissociates from For the understanding of substrate (Fig. 1). mechanism of unwinding it is of importance to know whether this dissociation occurs in an ATP-bound state of the protein or in a non-ATP-bound state or in both Experimentally, this question can be accessed by measuring the effect of ATP concentration variation on the reaction amplitude. Decreasing reaction amplitudes with decreasing ATP concentrations would indicate that dissociation in non-ATP-bound occurs а Dissociation in an ATP-bound state would be indicated by differences in the reaction amplitudes with duplexes of different length under ATP saturation of the system. Measurements conducted of the reaction amplitude dependence on the ATP concentration with a 36bp substrate and a 83bp substrate (Fig. 5). The reaction amplitude decreased with decreasing ATP concentrations, indicating clearly that dissociation occurs at non-ATP bound states The differences in the reaction the protein. amplitude of both substrates near ATP saturation suggest further that the protein dissociates also in the ATPbound state. (Fig. 5).

10

15

20

25

30

Effect of  $Mg^{2+}$  substitution on the unwinding reaction. At the reaction conditions tested so far, the only response to the variation in the duplex length was the reaction amplitude. Although this suggests a processive unwinding reaction, the fact that no effect was found on the rates of the unwinding reaction indicates that not a potential translocation limits the overall rate of the However, for the quantification of reaction. unwinding steps in terms of the step size and individual rate constants it is necessary that the translocation directly affects the reaction rate. Therefore, attempts were made to decrease the rate of translocation relative to the rate limiting step such that intermediates of the unwinding reaction would be kinetically detectable and translocation would be directly reflected unwinding timecourse (Fig. 1). Variation in pH and temperature did not result in the desired changes in the Subsequently, we examined timecourses (not shown). whether a substitution of  $Mg^{2+}$  with other divalent cations, which act as cofactor for the ATP hydrolysis, provides reaction conditions where the translocation would be slower relative to the previously rate limiting step. Recently, only Mn<sup>2+</sup> and Co<sup>2+</sup> were found substitute for Mg2+ in the unwinding reaction for NPH-II In reactions with RNA-protein pre-1992). annealing and in the presence of trap RNA,  $\mathrm{Mn}^{2^+}$  did not change the timecourses as compared to the reactions with However, substituting Mg<sup>2+</sup> with Co<sup>2+</sup>  $Ma^{2+}$  (Fig. 6). in a substantial change in the observed resulted timecourse (Fig. 6). With Co2+, the timecourse displayed a pronounced lag phase, suggesting reaction intermediates This assumption was supported by measuring (Fig. 1). reactions with substrates with duplex regions different length in the presence of Co2+. The timecourses

10

1.5

20

25

30

showed an increasing lag phase with increasing duplex duplex, the longer the the length, i.e. intermediates appear in the unwinding reaction (Fig. 7). This indicated that in the presence of Co2+, it can be directly observed that the reaction proceeds in distinct consecutive steps and can therefore be considered to be In accordance with the results described processive. above (Fig. 2 and 3), the reaction amplitude decreased with increasing duplex length (Fig. 7), indicating that protein dissociates more frequently during the unwinding of longer duplexes.

for probing substrates Employing multi-piece directionality of the unwinding reaction. The results described above (Figs. 2-7) suggested that the unwinding of RNA duplexes by NPH-II is in fact processive. second basic feature of the unwinding reaction, the directionality of the process, could not be accessed yet. monitoring the unwinding reaction with the described methods bears the disadvantage that observed unwinding is caused by an event at the end of the unwinding reaction (Fig. 1), no direct evidence for directionality can be provided. Although a processive unwinding together with the binding of the protein at the single stranded overhang of the substrate indirectly argues for a certain directionality of the process, a number of alternative unwinding mechanisms (for instance looping of the single-stranded-bound protein into the duplex region) cannot be ruled out. In order to prove directionality unambiguously, we attempted to employ a more direct assay, where, beside, the unwinding of the "whole" duplex at least one intermediate has to be monitored during the reaction. We accomplished that by designing multi-piece-substrates (MPS), which comprise a

10

15

20

25

30

regular bottom strand but two adjacent to each other binding top strand pieces (Fig. 8a). Provided that the two pieces can be separated from each other on native PAGE, it should be possible to observe the separate displacement of the two pieces as the translocates in a directional way. In order to exclude effects of the length of the different pieces per se, we designed two MPS; one with the longer piece next to the single stranded overhang, and another one with the shorter piece next to the single stranded overhang (Fig. The unwinding reactions were performed with protein-RNA pre-annealing and in the presence of trap RNA, such that dissociation of protein from the substrate was irreversible.

Both MPS were unwound by NPH-II, emphasizing that the helicase tolerates nicks in the top strand of the In the presence of Mg<sup>2+</sup>, both pieces were substrate. displaced with a similar rate (Fig. 8b). The piece binding more distal to the overhang was displaced with a lower amplitude as compared to the piece binding closer to the single stranded overhang. This was observed for both MPS, and, therefore, the amplitude effects are caused only by the position of the pieces relative to the These results support the findings with the regular substrates (Figs. 2,3), where, although more protein dissociates from the substrate with increasing duplex length, the reaction rate is not limited by the translocation. Moreover, the fact that the amplitude was lower for the piece more distal to the overhang but the reaction rates of both pieces were similar suggests that the event which limits the rate of the overall reaction is before the translocation process, i.e. the unwinding

10

15

20

25

30

initiation is likely to limit the overall reaction in the presence of  $Mg^{2+}$ .

In the presence of Co<sup>2+</sup>, the displacement of both pieces occurred with different lag phases (Fig. 8c). The lag for the pieces next to the overhang was always smaller, than the lag for the pieces more distal to the overhang (Fig. 8c), indicating that one piece is displaced after the other and that this displacement process has a directionality: initiating from the single stranded region the helicase translocates towards the other end of the duplex while it unwinds it. Moreover, the reaction amplitude for the piece more distal to the overhang was smaller then the amplitude for the piece next to the overhang, indicating that also in the presence of Co<sup>2+</sup> protein dissociates from the substrate more frequently with increasing duplex length.

#### Materials and Methods

NPH-II was expressed and purified as described (Gross and 1995). RNAs were prepared by Shuman, transcription of PCR-generated T7 transcription templates (Jankowsky and Schwenzer, 1996) or by chemical synthesis (Wincott et al., 1995). The PCR-amplified DNA templates represent a segment of the ampicillin-resistance gene of the pBS(+/-) phagemid (Stratagene). To generate perfect blunt-end duplexes, the RNA pieces were trimmed by sitedirected processing using engineered DNAzymes (Santoro and Joyce, 1997; Pyle et al., 2000) with 12 nucleotides on each of the binding arms. Bottom-strand RNAs were joined from two separately synthesized oligonucleotides by template-directed ligation using T4 DNA ligase (Moore and Sharp, 1992) RNA duplexes were formed by combining the botton-strand RNA with a five-fold molar excess of  $\gamma^{32}$ 

10

15

20

25

30

P-labelled top strand in 10mM MOPS, 6.5, 1mM EDTA. The solution was heated to 95°C for 2 min and cooled to room temperature over 90 min. Duplexes were separated from single-strand RNA by native PAGE, visualized by radiolytic scanning (Packard Instant Imager) and excised from the gel.

#### Unwinding reactions

Unwinding reactions were performed at room temperature in 30µl of 40mM Tris-HCl buffer, pH 8.0 and 4mM MgCl2 or CoCl2. The reaction also contained 25mM NaCl, which was introduced with the protein storage buffer. In a typical reaction, 1-2nM RNA substrate was incubated with 10-15nM NPH-II in reaction buffer without ATP at room temperature for 5-7 min. Longer pre-incubation time did not change the reaction kinetics. Saturation of substrate with protein before the reaction was verified by gel-shift analysis (Lohmann and Bjoernson, 1996). The unwinding reaction initiated by adding the ATP to concentration of 3.5mM unless otherwise stated. Aliquots at the respective time points were quenched with two volumes of stop buffer 25 mM EDTA, 0.4% SDS, 0.05% BPB, 0.05% XCB, 10% glycerol containing 200nM of unlabelled top-strand RNA to prevent re-annealing of unwound duplexes during electrophoresis. Reannealing of unwound duplexes during the reaction did not affect unwinding kinetics under any reaction conditions as verified by independent measurements of association rate constants of Excess RNA (Trap RNA) (200 nM the substrate strands. final concentration added with the ATP) was a singlestrand of 39-nucleotides of unrelated sequence. concentrations of trap RNA did not change observed reaction amplitudes.

10

15

20

25

30

Unwinding reactions were also monitored in real time using fluorescence energy transfer experiments on substrates labelled at the 3' and 5' ends of the duplex terminus farthest from the single stranded 3' overhang. These measurements were superimposable with results from gel-shift measurements and confirmed the first-order nature of the time courses as well as the rate constants.

## Kinetic analysis

Data were fit numerically using the FITSIM software package (Barshop and Frieden, 1983). Time courses were corrected for the reaction amplitudes, and initial kinetic parameters were determined using the KINSIM software (Barshop and Frieden, 1983). Unwinding step size and rate constants were determined from time courses in  $Co^{2+}$  using a kinetic model in which the unwinding reaction consists of N consecutive first-order reactions where N is the number of kinetic steps. Rate constants (except for the first step see below) were linked, that is, forced to yield the same value in the fitting. linked rate constants and the first rate constant were allowed to float simultaneously. On the basis of the observation than an initial step is slower than subsequent steps in  $Mg^{2+}$  (see Fig. 11b and text), the first kinetic step was defined as having a different rate constant  $(k_1)$  than subsequent kinetic steps  $(k_0)$ . Using this model, increasing numbers of steps (N) were examined iteratively for each duplex until  $k_{\scriptscriptstyle 1}$  and  $k_{\scriptscriptstyle u}$  approached constant values for the different duplexes. Convergence occurred when  $k_1 = 2.3 \pm 0.2 \text{ min}^{-1}$  and  $k_u = 13.4 \pm 0.8 \text{ min}^{-1}$ .

Note that  $k_{\rm u}$  is an apparent rate constant that depends on the ATP concentration according to  $k_{\rm u}=k_{\rm u[S]}$  [ATP/(ATP + K'\_{\rm d}), where  $k_{\rm u[S]}$  is the respective rate constant at ATP

saturation. The step size (m) was calculated according to m=L(N-y), where y is the number of kinetic steps do not contribute to the actual strand displacement and L is the duplex length. A step size of m=6 and a value of y=1 were consistently calculated for all duplexes  $\lambda$  including multi-piece substrates.

The lower limit for the translocation rate constant in  ${\rm Mg}^{2^+}$  was estimated by considering that a lag phase was not observed with the longest (83 bp) duplex (Fig. 9b). Assuming an unwinding step size identical to that in  ${\rm Co}^{2^+}$  (6 bp), and that  $k_u$  must be equal or greater than a value that does not cause an apparent lag phase in 14 unwinding steps, the translocation rate constant was estimated as  $k_u > ~350~{\rm min}^{-1}$ .

Equation (1) was derived from the expression describing the dependence of reaction amplitude (A) on the processivity (P):

# $A = (1 - x) P^{i/m}$

25

30

5

10

15

20

where  $\chi$  is the fraction of protein that dissociates from the substrate before unwinding occurs. P is then substituted with a term that relates processivity and ATP concentration under the conditions specified by the scheme in Fig. 13.

20

25

30

$$P = \frac{k_{\text{trist}} \left( \frac{|\text{ATP}|}{K_d' + |\text{ATP}|} \right)}{k_{\text{trist}} \left( \frac{|\text{ATP}|}{K_d' + |\text{ATP}|} \right) + k_{\text{F}} \left( 1 - \frac{|\text{ATP}|}{K_d' + |\text{ATP}|} \right)}$$

where  $K_d$  is the apparent dissociation constant of ATP from the enzyme substrate complex.

#### RNA Substrate Preparation

Chemical Synthesis: RNA oligonucleotides were prepared by chemical synthesis using phosphoramidite chemistry (amidites purchased from Glen Research) on an ABI 392 RNA/DNA synthesizer. Deprotection of the crude oligonucleotides was carried out according to standard protocols (Wincott et al., 1995). All RNA oligonucleotides were purified on denaturing PAGE.

The bottom strand RNAs were joined out of two separately synthesized oligonucleotides by template directed ligation using T4 DNA ligase (Moore and Sharp, 1992). The ligated products were purified on denaturing PAGE.

Fluorescent Labeling: Amino linkers were placed in the 3' or 5' position of the respective RNA during the synthesis. After removal of all deprotection groups, the modified RNA was labeled with fluorescein-or rhodamine-isothiocyanate (Sigma), respectively. Labeling reactions were carried out in the dark for 12-18 hours with 50 mM

dye-isothiocyanate and RNA concentrations below 50  $\mu$ M in 0.1 M sodiumbicarbonate (pH 9.0) and 20% (v/v) DMSO for the fluorescein-isothiocyanate labeling and 50% (v/v) DMSO for the rhodamine-isothiocyanate labeling. The excess rhodamine-isothiocyanate was removed by repeated phenol extractions followed by ethanol precipitation. The excess fluorescein-isothiocyanate was removed by repeated ethanol precipitations. All labeled RNAs were finally purified on denaturing PAGE.

10

15

20

25

30

5

transcription: RNAs for the multi-piece-Ιn vitro substrates were prepared by in vitro transcription of PCR generated templates (Chabot, 1992). The PCRamplified DNA-templates represent a segment of ampicillin resistance gene of the pBS (+/-) phageimid Templates for bottom and top strand RNAs (Stratagene). were separately amplified from ScaI linearized phageimid using different pairs of primers with the respective sense primer containing the binding sequence as well as the T7 promoter sequence.  $100\mu L$  PCR reactions were carried out for 30 cycles (52°C, 72°C, 94°C, 1 min each) followed by a 7 min final extension at 72°C. Homogeneity of the PCR products was verified on a 2% agarose gel. The PCR reaction solutions were extracted with an equal volume of phenol, followed by extraction with chloroform isoamylalcohol (Sambrook et al., 1989). Not incorporated Pharmacia). dNTPs were removed by SEC (NAP-5,Subsequently, the volume of the solution was reduced in a Speedvac concentrator (Savant). The obtained DNA templates were used for in vitro transcriptions with T7 polymerase according to standard procedures. transcribed RNAs were purified on denaturing PAGE.

10

15

2.0

25

30

The top strands for the Multi-Piece-Substrates were produced by site directed processing using an engineered DNAzyme (Santoro and Joyce, 1997). DNAzymes with 12 nucleotides in each of the binding arms were designed to cut at the desired positions. The DNAzyme reactions ( $10\mu$ M RNA,  $30\mu$ M DNAzyme) were carried out for 4h at  $40^{\circ}$ C followed by ethanol precipitation. Subsequently, the DNAzyme was destroyed by RQ RNAse free DNAse (Promega) in a  $100\mu$ L volume with 15units DNAse for 60 min at  $37^{\circ}$ C. The RNA was ethanol precipitated and the products were purified by denaturing PAGE.

Duplexes were formed by combining the bottom strand RNA with a 5 fold molar excess of labeled (either radioactively or fluorescently) top strand in 10mM MOPS (pH 6.5), 1mM EDTA. The solution was heated to 95°C and cooled to room temperature within 90 min. Duplexes were separated from single stranded RNA on native PAGE. The RNA was visualized either by UV-shadowing or by radiolytic scanning (Packard Instant Imager), cut out, eluted, and ethanol precipitated.

#### Helicase reactions

Unwinding reactions were carried out at room temperature in 40 mM Tris/HCl (pH 8.0) and 3mM MgCl<sub>2</sub>(MnCl<sub>2</sub>, CoCl<sub>2</sub>), 20mM NaCl was present in the reaction due to introduction with the protein storage buffer. In a typical reaction, 3nM RNA substrate was incubated with 10-15 nM NPH-II in reaction buffer without ATP at room temperature for 7 min. Longer incubation time did not change the observed reaction kinetics. The reaction was started by adding the ATP. In reactions with trap RNA, the trap was added together with the ATP at the reaction start.

10

15

20

25

30

Gel shift measurements: For the reactions monitored by gel shift PAGE, reactions were performed in a volume of 30  $\mu$ L. Aliquotes were taken at appropriate times and combined with two volume of stop buffer (25mM EDTA, 0.4% SDS, 0.05% BPB, 0.05% XCB, 10% glycerol), containing 200nM of unlabeled top strand in order to prevent reannealing of unwound duplexes during electrophoresis. Unwound strands were separated from intact substrate on native PAGE and the amount of unwound duplex was determined using a Molecular Dynamics PhosphorImager and the Imagequant Software.

Fluorescence Measurements: For the reactions monitored by fluorescence measurements, reactions were performed in fluorescence cuvette (600  $\mu$ L) in an Aminco SLM AB2 fluorescence spectrometer. Excitation wavelength was set at 492 nm, (8nm slid width) emission was recorded at 518 nm (8 nm slid width, PMT sensitivity 600-800V). The reaction was started as described and measurements were taken automatically in fixed intervals.

Employing a series of designed model substrates, it was shown than the unwinding of RNA duplexes by the DExH protein NPH-II is processive. In the presence of Mg<sup>2+</sup> the translocation does not limit the overall reaction rate. The rate-limiting step of the unwinding reaction is likely to be the unwinding initiation. The sensitivity of the reaction amplitude to the duplex length indicates that during each "unwinding step" a certain fraction protein dissociates from the substrate. The dependence of the reaction amplitude on the ATP concentration emphasizes that this dissociation occurs in non-ATP bound states of the protein as well as in ATP-bound states of the protein.

Also developed was an assay to test the directionality of the unwinding process and showed that the unwinding process has a defined directionality: initiating from the single stranded region the helicase translocates towards the other end of the duplex while it unwinds it. The proof of the processivity and directionality of the unwinding process is the prerequisite for quantitative characterization of the helicase reaction which is necessary to derive functional models.

#### References

Ali, J.A., and Lohmann, T.M. (1997) "Kinetic Measurement of the Step Size DNA Unwinding by Escherischia coli UvrD Helicase", Science, 275, 377-380.

5

Barshop, B. A. and Frieden, C. (1983) "Analysis of Numerical Methods For Computer Simulation of Kinetic Processes: Development of KINSIM--A Flexible Portable System. Anal. Biochem. 130, 134-145.

10

Chabot, B. (1992) "Synthesis and Purification of RNA Substrates, in RNA Processing: A Practical Approach", Higgins, S.J. and Hames, B.D. Eds., IRL Press, Oxford, U.K., pp 1-31.

15

de la Cruz, I., Kresler, D. and Linder P. (1999) "Unwinding RNA in Saccharomyces Cerevisiae: DEAD-Box Proteins and Related Families," Trends Biochem. Sc. 24, 192-198.

20

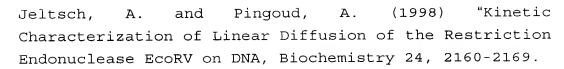
Gross, C.H. and Shuman, S. (1995) "Mutational Analysis of Vaccinia Virus Nucleoside Triphosphate Hydrolase II, a DEXH Box RNA Helicase", J. Virol., 69, 4727-4736.

25

Gross, C.H. and Shuman, S. (1996) "Vaccinia Virus RNA Helicase: Nucleic Acid Specificity in Duplex Unwinding, J. Virol, 70, 2615-2619.

30

Jankowsky, E. and Schwenzer, B. (1996) "Efficient Improvement of Hammerhead Ribozyme Mediated Cleavage of Long Substrates by Oligonucleotide Facilitators" Biochemistry 37, 15313-15321.



- 5 Kadare, G. and Haenni, A. L., (1997) "Virus encoded RNA Helicases," J. Virol 71, 2583-2590.
- Kelemen, B. R. and Raines, R. T. (1999) "Extending the Limits to Enzymatic Catalysis: Diffusion of Ribonuclease A in One Dimension" Biochemistry 27, 5302-5307.
  - Lohmann, T. M. and Bjoernson, K.P. (1996) "Mechanism of Helicase Catalyzed DNA Unwinding", Annu. Rev. Biochem. 65, 169-214.
  - Moore, M.J. and Sharp, P.A. (1992) "Site Specific Modification of Pre-Messenger RNA-the 2'-Hydroxyl Groups at the Splice Sites", Science, 256, 992-997.
- Pyle, A. M., et al., (2000) "Using DNAzymes to Cut, Process and Map RNA Molecules For Structural Studies or Modification" Methods Enzymol 317, 140-146.
- Santoro, S.W. and Joyce, G.F. (1997) "a General Purpose RNA-Cleaving DNA Enzyme", Proc. Natl. Acad. Sci., USA, 94, 4262-4266.
  - Schnapp, B. Molecular Motors, (1995) "Two Heads Are Better Than one" Nature 373, 655-666.
- Shimamoto, N. (1999) "One-Dimensional Diffusion of Proteins Along DNA, J. Biol. Chem. 274, 15239-15296.

Shuman, S. (1992) "Vaccinia Virus RNA Helicase: Ar Essential Enzyme Related to the DE-H Family of RNA Dependent NTPases", Proc. Natl. Acad. Sci. USA, 89, 10935-10939.

5

Shuman, S. (1993) "Vaccinia Virus RNA Helicase, J. Biol. Chem., 268, 11798-11802.

10

Staley, J. P. and Guthrie, C. (1998) "Mechanical Devices of the Spliceosome: Motors Clocks Springs and Things" Cell 90, 1041-1050.

15

Wagner, I.D.O., et al., (1998) "The DEAH-Box Protein Prp 22 is an ATPase that Mediates ATP Dependant mRNA Release From the Spliceosome and Unwinds RNA Duplexes," EMBO J. 17, 2926-2937.

Wincott et al. (1995) "Synthesis, Deprotection, Analysis and Purification of RNA and Ribozymes", Nucleic Acids Res., 23, 2677-2684.

20

Xiang, Q., et al., (1998) "Sequence Specificity of a Group II Intron Ribozyme: Multiple Mechanisms For Promoting Unusually High Discrimination Against Mismatched Targets" Biochemistry 37, 3839-3849.

25

Zimmeric, C. and Frieden, C. (1998) "Analysis of Progress Curves by Simulations Generated by Numerical Integration" Biochem. I. 258, 381-387.